COMPARATIVE ANALYSIS OF NUMERICAL COMPUTATIONAL TECHNIQUES FOR DETERMINATION OF THE WIND TURBINE AERODYNAMIC PERFORMANCES

by

Bojan M. PERIĆ[a]*, Aleksandar M. SIMONOVIĆ[a], and Miloš D. VORKAPIĆ[b]

[a] Department of Aerospace Engineering, Faculty of Mechanical Engineering, University of Belgrade, Belgrade, Serbia
[b] ICTM – CMT, University of Belgrade, Belgrade, Serbia

Original scientific paper
https://doi.org/10.2298/TSCI200216175P

The purpose of this paper is to explore and define an adequate numerical setting for the computation of aerodynamic performances of wind turbines of various shapes and sizes, which offers the possibility of choosing a suitable approach of minimal complexity for the future research. Here, mechanical power, thrust, power coefficient, thrust coefficient, pressure coefficient, pressure distribution along the blade, relative velocity contoure, at different wind speeds and streamlines were considered by two different methods: the blade element momentum and CFD, within which three different turbulence models were analyzed. The estimation of the mentioned aerodynamic performances was carried out on two different wind turbine blades. The obtained solutions were compared with the experimental and nominal (up-scaled) values, available in the literature. Although the flow was considered as steady, a satisfactory correlation between numerical and experimental results was achieved. The comparison between results also showed, the significance of selection, regarding the complexity and geometry of the analyzed wind turbine blade, the most appropriate numerical approach for computation of aerodynamic performances.

Key words: *wind turbine blades, blade element momentum, aerodynamic performances, CFD*

Introduction

Efficiency, cost, and calculation time are highly important in the design and manufacturing of wind turbine blades. Many companies tend to engage in computational analysis using different numerical models because the usage of high performance computational hardware helps overcoming expensive experiments in a faster and more accurate way [1].

Considering the aforementioned, significant papers have been published with the purpose of comparing different numerical methods for obtaining aerodynamic loads. The increase in the diameter of the wind turbine blade in order to enhance the power generation capacity leads to various aerodynamic phenomena which is important for the blade design. Detail information of flow separation, aerodynamic loads and wake development are important for the wind turbine designers to optimize the blade design. On the other hand, the calculation time and efficiency during design phase of the blade is essential. Considering these facts, various numerical studies have been formulated and improved [2-10].

* Corresponding author, e-mail: bojan.peric24@gmail.com

Generally, four types of aerodynamic models are employed in the previously mentioned references: blade element momentu (BEM), vortex, actuator type, and CFD. The main characteristics of the aerodynamic model comparison are accuracy, computational speed, the requirement of air-foil aerodynamic data, and the inclusion of viscous effects. Numerical models not only allow design engineers to gain the aerodynamic characteristic of the wind turbine blades, but they also facilitate this in a more efficient and convenient way using the main characteristics of the aerodynamic models. Using different numerical models, the parameters of wind turbine blade can be estimated or underestimated depending on the aerodynamic model that is used. Combining these numerical methods, design engineers have the possibility to model the turbulence in a better way.

In order to predict aerodynamic performance and flow field around the wind turbine blade in this study two approaches BEM and CFD are considered.

For these reasons, two blades for offshore and onshore wind turbines of significantly different rotor sizes have been investigated. Comparative analyses of aerodynamic performances of the wind turbine rotors named DTU 10 MW RWT (Denmark Technical University 10 MW Reference Wind Turbine) blade and MEXICO blade were performed [11, 12]. For both blades, one-equation Spalart-Allmaras (SA), two-equation k-ω SST, and four-equation transition SST turbulence models were employed. The aim of this paper is to list and compare possible numerical approaches for aerodynamic computation of the wind turbines of different sizes functioning in different conditions. By choosing an adequate model, satisfactory estimations of mechanical power, thrust, power coefficient, thrust coefficient, pressure distribution along the blades, relative velocity contoure at different wind speeds, as well as their comparison with the experimental and reference data can be attained.

The main contributions and novelties of this study are the examination, validation, comparison and definition of the limitations of commercially available software suitable for the wind turbine aerodynamic analysis. Many research papers investigate only one of these blades [13-17] without performing a comparative analysis that accounts for the differences in small and large-scale blades. This paper clearly lists both the advantages and disadvantages of the two computational approaches, as well as the estimation of the possible accuracy of results, thus enabling engineers to choose a computational model of minimal complexity necessary for their own research. The value of the paper is also reflected in the investigation of *non-optimal* working conditions (*i.e.* at low or high wind speeds) on two very different geometries. Due to the enormous differences in size, the applicability of the two tested approaches to a wider range of Reynolds numbers has also been examined.

Model description

The DTU 10 MW RWT, fig. 1(a), was designed by up-scaling the NREL 5 MW reference turbine at the Technical University of Denmark (DTU) to the rated power of 10 MW.

On the other hand, the MEXICO, fig. 2(b), wind turbine blade is experimental, benchmark, pitch-regulated wind turbine that was designed within the EU under the project MEXICO and thoroughly tested at the German-Dutch wind tunnel in the Netherlands.

The DTU 10 MW RWT

This turbine is a traditional, three-bladed, both pitch and speed regulated, upwind wind turbine for offshore sitting. This work investigates the behavior of the DTU 10 MW RWT blade in the range of wind speeds V_0 = 5-25 m/s. For the DTU 10 MW RWT wind tur bine mechanical power, thrust force, power coefficient, thrust coefficient, flow field, and

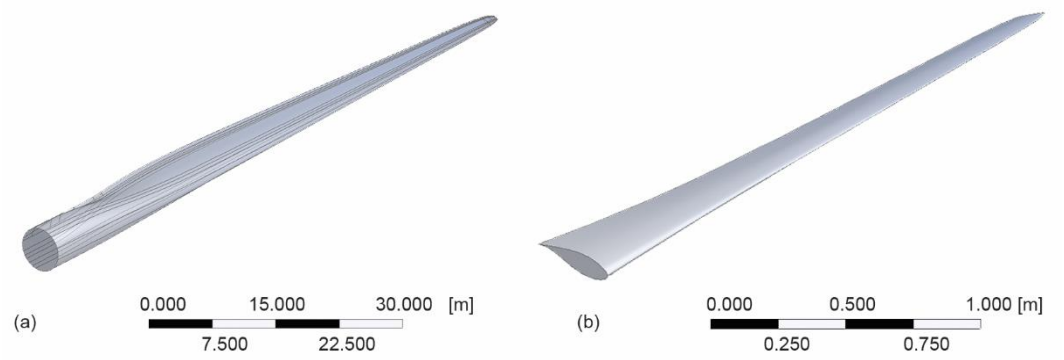

Figure 1. The 3-D geometric models of wind turbine blades; (a) DTU 10 MW RWT blade and (b) MEXICO wind turbine blade

blade pressure distribution were analyzed. The key parameters necessary for the turbine computation are: rotor radius R = 89.15 m, minimum rotor rotational speed ω = 6.0 rpm, maximum rotor rotational speed ω = 9.6 rpm, pitch angle varying from θ_0 = 0° to θ_0 = 22.975°, cut-in wind speed V_{cut} = 4 m/s and cut-out wind speed V_{out} = 25 m/s. The blade geometry includes air-foils of FFA-W3 series, starting from the blade root with FFA-W3-600GF, FFA-W3-480GF, FFA-W3-360, FFA-W3-301, FFA-W3-241 to the tip of the blade with NACA 0015. Additional information for the DTU 10 MW RWT can be found in [11].

The MEXICO wind turbine

As well as for the DTU 10 MW RWT, for the MEXICO wind turbine mechanical power, thrust force, power coefficient, thrust coefficient, flow field, and blade pressure distribution were analyzed at different wind speeds in the range V_0 = 10 m/s and 30 m/s and two different rotor angular velocities: ω = 324.5 rpm and ω = 424.5 rpm. The diameter of this 3-bladed, horizontal-axis wind turbine is D = 4.5 m. The details for the MEXICO wind turbine can be found in [1, 12]. The blade includes three types of air-foils, DU91-W2-250, RISØ-A1-21 and NACA 64-418. All of the simulations in this work are carried out with a constant pitch angle of θ_0= −2.3°, rotational speed of ω = 324.5 rpm, constant air density of ρ = 1.225 kg/m^3 in the pure axial flow (no yaw).

Numerical methods

The computations of the aerodynamic performances of both MEXICO wind turbine blade and DTU 10 MW RWT blade by BEM and FVM (finite volume method) are performed using QBLADE software and ANSYS Fluent.

The BEM modeling

The QBLADE [18] is an open-source software for the simulation and design of both vertical- and horizontal-axis wind turbines. This software includes the BEM method, double multiple streamtube (DMS) and non-linear lifting line theory (LLT). To compute the wind turbine blade aerodynamic characteristics using the BEM, QBLADE is coupled with XFOIL code for air-foil import and analysis. The XFOIL code [19] is a standard analysis tool for air-foils validated numerous times [20]. The QBLADE has modules for air-foil design and analysis, ex-

trapolation of lift coefficient, C_l, drag coefficient, C_d, and moment coefficient, C_m, to $\alpha = 360°$ angle of attack (AoA), blade design and optimization and turbine definition and simulation.

Estimation of the aerodynamic performance of the DTU 10 MW RWT and MEXICO blade using QBLADE started with the import of air-foils geometries. The aerodynamic characteristics, C_l, C_d, and C_m, for the local values of Reynolds numbers Re = $6\cdot10^6$, Re = $10\cdot10^6$, and Re = $12\cdot10^6$ for the DTU 10 MW RWT blade and $0.29\cdot10^6 \leq \text{Re} \leq 0.51\cdot10^6$ for the MEXICO blade are calculated in the range of AoA from −32° to +32° by the panel method and then extrapolated to the range from −180° to +180°. For both blades, constant air density of $\rho = 1.225$ kg/m^3 was set, all air-foil polar Mach number M = 0 was assumed, *i.e.* the compressibility effects were not considered. The aerodynamic calculations were performed for the range of wind speeds V_0 = 5-25 m/s for both blades. Rotor rotational speed varied from 6-9.6 rpm and the pitch angle from 0°–22.975° for the DTU 10 MW RWT blade according to the control strategy given by [11]. In this work, the simulations for the MEXICO blade are carried out with a constant pitch angle of −2.3° and rotational speed of 324.5 rpm [12].

The obtained values of mechanical power, P, thrust force, T, power coefficient, C_P, and thrust coefficient, C_T, are compared with the reference data for the DTU 10 MW RWT, figs. 4-7. The same process is repeated for the MEXICO blade.

The BEM model represents a combination of the blade element theory and momentum theory. Applying the BEM model involves dividing the blade into several independent segments and computing the forces, acting on each segment *i.e.* requires aerodynamic air-foil data. Each blade segment is represented by a suitable air-foil whose AoA dictates the values of the local lift and drag coefficients. Summing the loads, *i.e.* normal and tangential forces, as well as the forces of drag and lift for each segment produces the total load. In order to include the finite number of blades of the real rotor similar to [21], a correction factor is defined.

In order to include the finite number of blades of the real rotor the correction factor is defined. Since the pressure on the upper surface is lower than the pressure on the lower surface, this leads to the reducing of the lift near the tip of the blade. There are numbers of methods for including the effect of the tip loss. Prandtl proposed a relatively simple method, modelling the wake of the wind turbine as vortex sheets. In this paper, the correction factor is calculated using QBLADE software in the simulation settings and Prandtl tip loss was used. The correction factor, F, based on Prandtl's method is:

$$F = \left(\frac{2}{\pi}\right)\cos^{-1}\left(\exp\left\{-\left[\frac{\frac{B}{2}\left(1-\frac{r}{R}\right)}{\frac{r}{R}\sin\varphi}\right]\right\}\right) \tag{1}$$

where B is the correction factor (always between 0 and 1) represents the function of a number of blades, φ – the angle of relative wind, and r/R – the position on the blade. This tip loss correction factor characterizes the reduction in the forces at a radius, r, along the blade that is due to the tip loss at the end of the blade.

Than the lift coefficient becomes:

$$C_l = 4F\sin\varphi\frac{(\cos\varphi - \lambda_r\sin\varphi)}{\sigma'(\sin\varphi + \lambda_r\cos\varphi)} \tag{2}$$

where σ' is the local rotor solidity and λ_r – the $\lambda_r$local speed ratio.The tip loss correction factor affects the forces derived from momentum theory.

The main shortcomings of the BEM model are: flow steadiness assumption, incapability of providing detailed information on the flow field, and only a partial consideration of viscosity effect. On the other hand, the BEM model quickly provides sufficiently accurate results for working regimes close to nominal [22]. With respect to the mentioned advantages and disadvantages, BEM is used for comparison and as a preliminary design tool in this study.

The CFD modeling

Given that the BEM cannot provide detailed information on the flow visualization and wake modeling, CFD is also considered as an important and the most common approach to the design and prediction of the aerodynamic performances of wind turbine blades. Due to the fact that modern wind turbine blades have a complex geometry and numerous flow phenomena being present, such as the dynamic stall, flow separation, *etc.*, flow field is difficult to simulate. One of the advantages of the CFD model is the ability to provide the results of higher levels of accuracy compared to the BEM, vortex, and actuator type model. The main disadvantages are that it requires a lot of time and resources for computation. Because of its increased accuracy and possibility to obtain complete data on the flow surrounding the blades, the CFD model was chosen as the second model for estimation of aerodynamic performances of the blades. So, in order to provide wind turbine wake aerodynamics and appropriate visualization around the blade with the possibility of using different viscous models the Navier-Stokes equations have to be solved. The 3-D, time-dependent, RANS equations are discretized using a finite volume approach.

Computational domain and boundary conditions

Since air-flow around the DTU 10 MW RWT blade and MEXICO blade are assumed axisymmetric, the fluid domain is modeled as follows. In order to reduce the simulation time, the computational domain was formed using a single blade in a 120° radial stream tube domain segment, fig. 2(a). The hub and tower geometries were not considered at this stage. Fluid domain is in the shape of a 1/3 rotational frustum. The smaller, top base with a 6*R* radius is located 6*R* upstream from the blade, while the outlet, greater base with a 20*R* radius is placed 20*R* downstream from the blade.

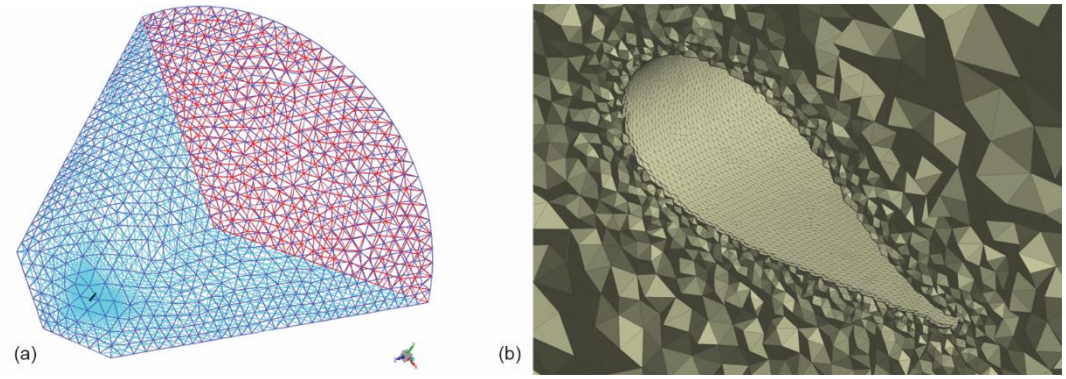

Figure 2. Generated computational mesh of DTU 10 MW RWT blade; (a) whole domain and (b) region around a cross-sectional air-foil

The boundary conditions are: velocity is assigned to the two (frontal and lateral, conical) inlet surfaces, pressure equal to the atmospheric is prescribed along the only outlet surface,

the two longitudinal faces form a periodic interface, and the wind turbine blade surface is considered as a no-slip rotating wall. Frame motion is assigned to the whole computational domain.

Mesh

For both blades, fluid domain is meshed with unstructured hybrid mesh. Twenty prismatic layers surround the blade surfaces for better calculation accuracy and resolution of the boundary-layer, fig. 2(b). Non-dimensional wall distance for the DTU 10 MW RWT blade is $y^+ < 5$ for all turbulence models. For the MEXICO blade non-dimensional wall distance is $y^+ < 1.5$. The mesh is additionally refined in a spherical zone of $1.3R$ diameter encompassing the both blades.

In order to validate the cell size at the DTU 10 MW RWT blade surfaces, the computed power as a function of the total number of elements was investigated, fig. 3. In this case, three parameters are set: wind speeds are V_0 = 5, 11, and 25 m/s, rotor rotational speeds are ω = 6, 8.836, and 9.6 rpm and pitch angles are θ_0 = 1.966°, 0°, and 22.975°. Four cell face sizes at the blade surfaces are investigated, *i.e.* 0.4, 0.2, 0.1, and 0.09 mm.

Figure 3 shows that power converges at the mesh size of 0.1 mm. Further refinement of the mesh size to 0.09 mm only results in 2.14% relative difference, with the increase in the total number of elements from 8.2 million to 10 million, which significantly increases the computational time. For these reasons, the mesh size of 0.1 mm is chosen as the appropriate cell face size at the blade surfaces.

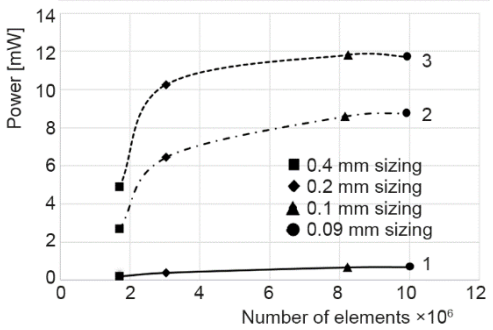

Figure 3. Mesh convergence study with respect to the computed mechanical power; *1 – convergence line V = 5 m/s, 2 – convergence line V = 11 m/s, 3 – convergence line V = 25 m/s*

Mesh validation of the MEXICO blade was performed by using power as a function of the total number of elements on the similar way as the DTU 10 MW RWT blade. Three wind speeds are set, V_0 = 10, 15, and V_0 = 24 m/s, rotor rotational speed ω = 324.5 rpm and pitch angle $\theta_0 = -2.3°$. Three cell face sizes at the blade surfaces are investigated, *i.e.* 5, 8, and 10 mm. The power converges with 2.7 million cells using 8 mm mesh size at the blade surface with 2.9% relative difference in comparison with expected results.

Turbulence models

In this study, three turbulence models are used: the one-equation SA, two-equation *k-ω* SST, and four-equation transition SST model.

The SA model solves one transport equation for the eddy viscosity [23]. This model gives reasonable results for a large variety of flow problems [24].

The *k-ω* SST model is widely used for field-tests of the wind turbine blades. This model represents an improvement of the baseline *k-ω* model and accounts for the turbulence shear stress transport when computing turbulent viscosity [25, 26].

The transition SST model represents coupling of the *k-ω* SST model transport equations with two additional transport equations governing the transitional region around the blade [25]. Hence, it is particularly developed for flows including zones of both laminar and turbulent flow.

Numerical schemes and convergence criteria

Numerical simulations for both blades were performed in ANSYS FLUENT v16.2. RANS equations were used with SA, *k-ω* SST and transition SST model. Air (fluid) was considered as incompressible gas of constant dynamic viscosity. The imposed zonal and boundary conditions are the rotational effects in the form of additional terms in the equations considered in the whole computational domain (steady frame of reference computational approach), wind velocity and corresponding turbulent quantities assigned to the two inlet (frontal and outer) surfaces, equaling of the atmospheric pressure defined along the outlet surface, two lateral/longitudinal faces form a periodic interface and wind turbine blade surfaces considered as a no-slip rotating wall.

The pressure-based SIMPLEC scheme is used for the pressure-velocity coupling. Gradients are estimated by the least squares cell-based method. Spatial discretization schemes are of the second order. The computations were performed until reaching converged values of power and thrust coefficients, usually between 1500 and 3000 iterations [27].

Results and discussion

Since models that differ in complexity and starting assumptions were compared, there are also differences in the results they are able to provide. The simpler BEM model generally provides the values of global parameters, while the CFD approach provides insight into the complete flow field around the blades.

During the calculations of aerodynamic performances, the computer with Intel Xeon E5-1620 v3, 3.5 GHz (8 CPU) processor, Fujitsu, (CELSIUS M740) motherboard, NVIDIA Quadro K620 graphic controller, 32 GB of RAM and 2TB hard disk was used for numerical calculations.

The calculation time for the DTU 10 MW RWT blade according to the different turbulent models was different for all models. For one-equation SA the calculation time was six hours, for two-equation *k-ω* SST 9 hours, and for four-equation transition SST 11 hours.

The calculation time for the MEXICO blade was different than for the DTU 10 MW RWT blade due to a simpler blade geometry. The calculations were completed faster, specifically for one-equation SA the calculation time was five hours, for two-equation *k-ω* SST seven hours, and for four-equation transition SST nine hours. The times of eight hours are practically the same for both blades concerning the calculations done using BEM model.

Computed numerical results of the MEXICO and DTU 10 MW RWT blade are compared to the available experimental and nominal (up-scaled) values. The mechanical power and thrust curves as functions of wind speed for experimental and computed values by BEM, SA, *k-ω* SST, and transition SST turbulent models are shown in figs. 4 and 5. The obtained power coefficient, C_P, as a function of tip speed ratio, λ, thrust coefficient, C_T, as a function of tip speed ratio, λ, are shown in figs. 6 and 7. Flow field around and pressure distribution along the DTU 10 MW RWT and MEXICO blades for wind speeds: V_0 = 5 m/s, V_0 = 11 m/s, and V_0 = 25 m/s and for wind speeds: V_0 = 8, 12, and 24 m/s are illustrated in fig. 8.

Considering the presented power and thrust curves, it can be concluded that the simpler and computationally more efficient BEM model provides accurate results for lower wind speeds, figs. 4 and 5. In the cases of the DTU 10 MW RWT and MEXICO blades the applicable ranges of wind speeds are between 5-10 m/s and 5-13 m/s, respectively. Although the investigated geometries are different, somewhat reduced accuracy of the BEM when used for

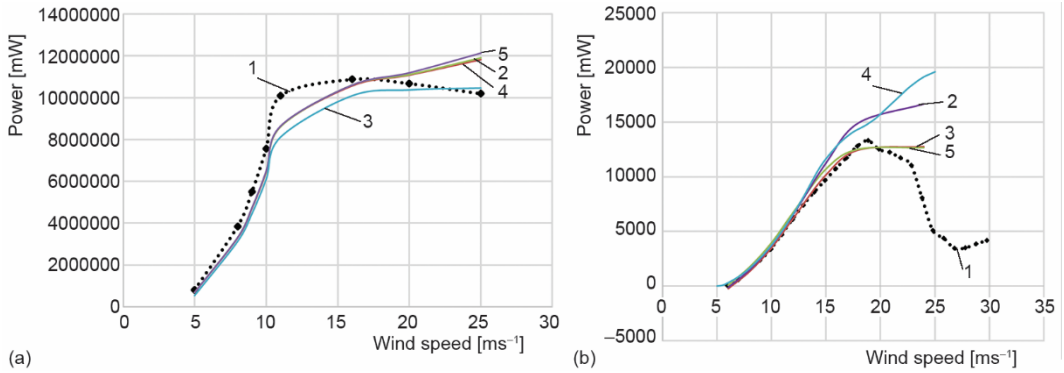

Figure 4. Comparison of computed mechanical power, *P*, as a function of wind speed for (a) DTU 10 MW RWT blade, *1 – DTU 10 MW RWT, 2 – transition SST, 3 – QBLADE, 4 – K-omega SST, 5 – SA* **and (b) MEXICO blade,** *1 – MEXICO rotor, 2 – SA, 3 – K-omega SST, 4 – QBLADE, 5 – transition SST*

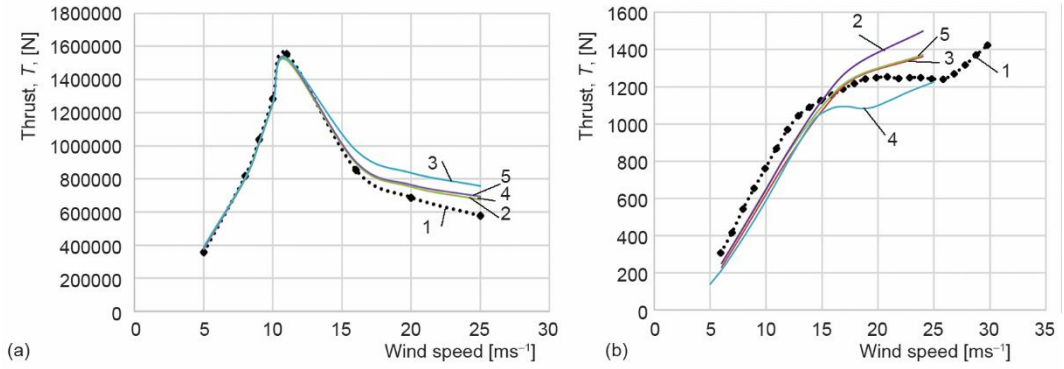

Figure 5. Comparison of computed thrust force, *T*, as a function of wind speed for (a) DTU 10 MW RWT blade, *1 – DTU 10 MW RWT, 2 – transition SST, 3 – QBLADE, 4 – K-omega SST, 5 – SA***, and (b) MEXICO blade,** *1 – MEXICO rotor, 2 – SA, 3 – K-omega SST, 4 – QBLADE, 5 – transition SST*

computation of tangential force (and hence power) acting on the DTU 10 MW RWT blade can also be explained by much higher values of Reynolds numbers and the inability of the computational model to adequately include these effects. More precisely, the observed divergence in the results is probably a consequence of the assumed air-foil characteristics. It must be noted that the greatest part of the DTU 10 MW RWT blade operates under 8-16 MRe, while the MEXICO blade undergoes 0.4-0.5 MRe, meaning that the values of Reynolds number for the DTU 10 MW RWT are approximately 20-30 times higher than for the MEXICO blade. At higher wind speeds, the obtained values of power and thrust deviate even more from the nominal/experimental values. This is particularly obvious for the MEXICO blade that does not change its collective pitch with wind speed in the course of the experiment. In the case of the DTU 10 MW RWT blade that is both pitch and speed-controlled, the differences between computed and nominal values are less significant and curve trends are reproduced better. All these findings confirm previously known presumptions that the applicability of the BEM model is limited to *nice* (nominal) flow cases that do not include any kind of flow phenomena (*e.g.* flow separation).

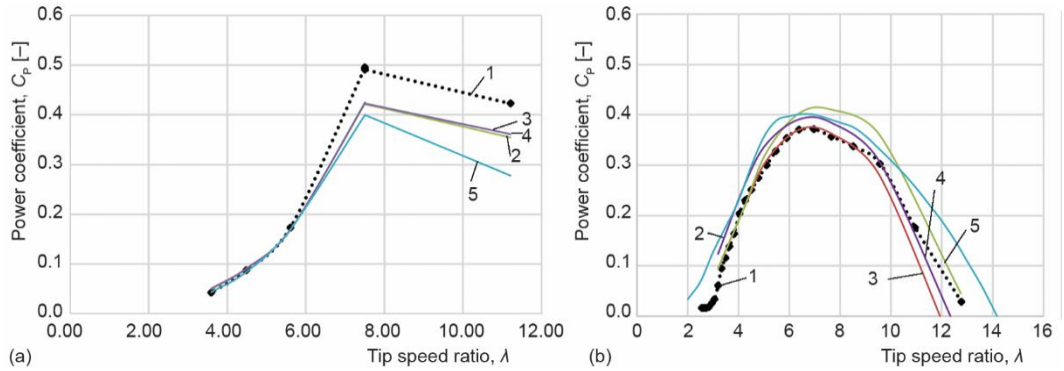

Figure 6. Comparison of computed power coefficient, C_P, as a function of tip speed ratio, λ, for (a) DTU 10 MW RWT blade, *1 – DTU 10 MW RWT, 2 – transition SST, 3 – QBLADE, 4 – K-omega SST, 5 – SA*, **and (b) MEXICO blade,** *1 – MEXICO rotor, 2 – SA, 3 – K-omega SST, 4 – QBLADE, 5 – transition SST*

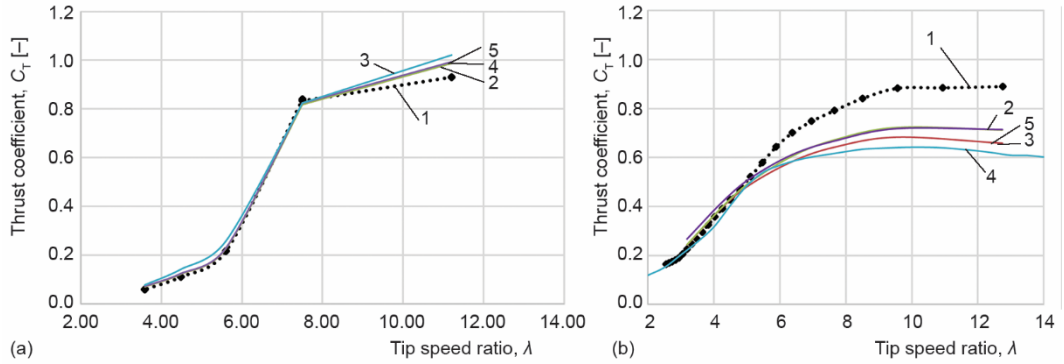

Figure 7. Comparison of computed thrust coefficient, C_T, as a function of tip speed ratio, λ, for (a) DTU 10 MW RWT blade, *1 – DTU 10 MW RWT, 2 – transition SST, 3 – QBLADE, 4 – K-omega SST, 5 – SA*, **and (b) MEXICO blade,** *1 – MEXICO rotor, 2 – SA, 3 – K-omega SST, 4 – QBLADE, 5 – transition SST*

As expected, the RANS approach provides values, which better match the nominal/experimental results obtained for both of the considered blades. The observed inconsistencies are partially the consequence of neglecting all other elements except the blades in the simulations as well as the adopted single-frame-of-reference approach that assumes a fictional rotation of the complete domain (this is the simplest, steady computational technique applicable to rotating flows). From the three studied turbulence models used for the closure of flow equations, the SA seems the least accurate for these kinds of rotational flows, while the *k-ω* SST and transition SST provide very similar results implying that the investigated flows are predominantly turbulent and that there is no particular need to use the much more computationally expensive transition model.

Taking into account the significantly increased computational time and effort, the greatest advantage of the RANS approach used with the *k-ω* SST model over the BEM approach is the widened range of wind speeds at which the rotor flow can be simulated. In this case, wind speeds up to 20 m/s (which correspond to approximately 80% of the possible operational regimes) can be considered with satisfactory accuracy. This means that by using CFD in blade design, more efficient and improved rotors can be achieved.

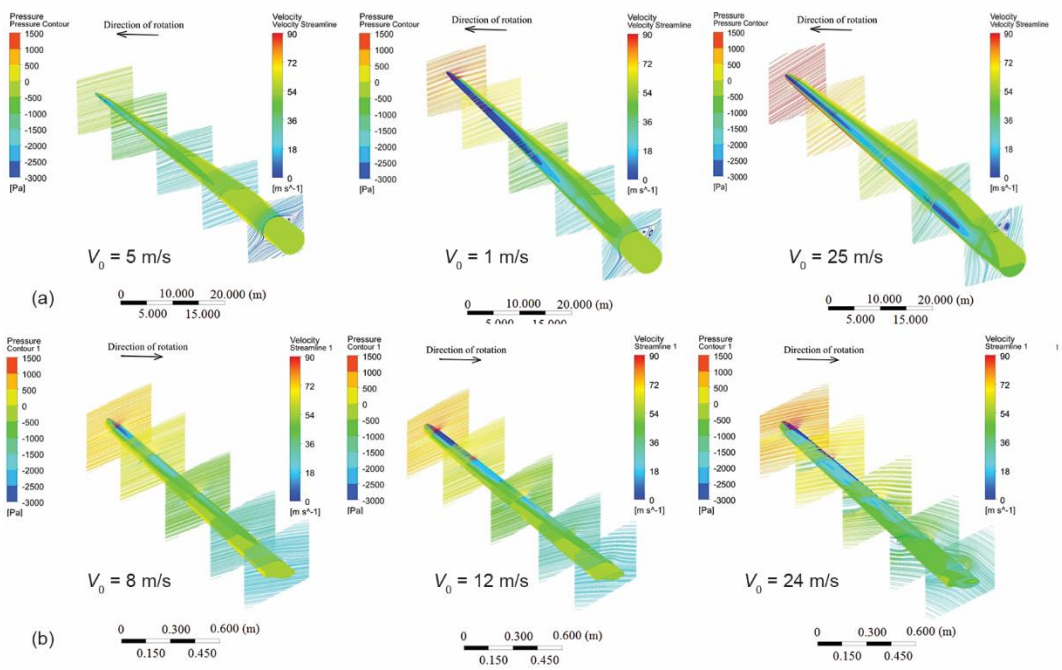

Figure 8. Flow field around and pressure distribution along the blade for different wind speeds for (a) DTU 10 MW RWT blade and (b) MEXICO blade

In order to compare rotors of different scales and draw general conclusions on the applicability of considered computational approaches, it is also convenient to illustrate power and thrust coefficient curves with the respect to tip-speed-ratio, λ, figs. 6 and 7. Optimal tip-speed-ratio for both rotors is around 7. All tested numerical models reproduce well the trends/shapes of the coefficient curves.

However, considering the DTU 10 MW RWT blade, it is now more evident that all three turbulence models provide quite similar non-dimensional results. When these enormous wind turbine scales are in question, any of them can be used to achieve accuracy of 15% (compared to the nominal power coefficient), while both computational approaches provide underestimated prediction of power coefficient. On the other hand, the thrust coefficient values computed by both BEM and CFD models show better agreement to the nominal values.

For the MEXICO blade, outcome is slightly different. Although all computational models overestimate the power coefficient, the *k*-ω SST seems to be able to provide the results of 5% accuracy in the range of wind speeds between 8-18 m/s which corresponds to tip-speed-ratio in bounds [4-9]. Also, all computational models underestimate thrust force coefficient with the discrepancy from experimental values reaching approximately 20%. The values of tip speed ratio for the DTU 10 MW RWT blade for all numerical models show good matching with the referent values. For the MEXICO blade, discrepancy of the thrust force coefficient during the comparison to the experimental data shows significant difference for higher values of tip speed ratio. Another way of testing is the comparison of distributions of normal force along the blade. The diagrams of distributions of normal force for this blade, as well as the above-mentioned discrepancy in the thrust force coefficient using different models can be found in the paper [28].

In order to visualize the flow fields around the blades the CFD model is employed. Five different cross sections located along the blades at relative longitudinal co-ordinate y/R = [0.1, 0.3, 0.5, 0.7, 0.9] for the DTU 10 MW RWT blade and y/R = [0.2, 0.4, 0.6, 0.8, 0.9] for the MEXICO blade are chosen for streamline illustration while the surface of the blade is colored according to the pressure distribution computed by the k-ω SST model. For comparison of the flow fields at different operational regimes roughly corresponding to cut-in, optimal and cut-out cases, three wind speeds are chosen for both blades and investigated in more detail. Flow fields around the DTU 10 MW RWT blade at V_0 = 5, 11, and 25 m/s and flow fields around the MEXICO blade at V_0 = 8, 12, and 24 m/s are plotted in fig. 8.

While relative velocity increases along the blade, maximum tip-speeds for the DTU 10 MW RWT and MEXICO blades are 90 m/s and 76 m/s, respectively. Considering the DTU 10 MW RWT blade, although the pressure distribution becomes more emphasized with an increased wind speed (observe the expansion of the under-pressure zone along the leading edge of the upper blade surface colored in blue), the flow remains attached along the operational, streamlined part of the blade due to the good congruence of blade pitch and angular velocity. Flow separation can only be observed in the first cross-section around a circular root shape and its wake increases at higher wind speeds.

Again, for the MEXICO blade, results are somewhat different. While at lower and optimal wind speeds the flow remains attached, a significant flow instability along the whole surface of the blade can be observed at the high wind speed of 24 m/s, which explains the considerable deviation of the numerical results from the experimental values at this particular flow regime.

Conclusions

This paper summarizes the findings of comparative computational studies of the wind turbine blade aerodynamic performances. Two, different approaches, the BEM and RANS equations used by three turbulence models, have been implemented and the obtained results compared to the available reference or experimental data. The simulations are performed on the two blades primarily different in size and also in the blade shape and turbine control strategy.

As generally recognized, the frame of reference approach has the advantage of a much shorter computational time. The results show a very good matching with nominal and experimental values of the blades. The presented methodology could be used for initial performance estimation. The k-ω SST turbulence model employed in this numerical approach is important for an accurate prediction of the aerodynamic performances of the wind turbine blade as it matches satisfactorily to the nominal values. Rated wind speed, around 11 m/s, obtained by computation corresponds to the reference value.

It is demonstrated that both approaches can be used in preliminary design phases since they can provide results of 15% accuracy compared to the referent values of the 10 MW RWT blade and 6% accuracy compared to the MEXICO blade experiment values. Regardless of the blade scales and Reynolds numbers, the BEM model is limited to lower wind speeds, approximately up to 10, 12 m/s, while the CFD approach enables performing simulations of the improved precision for an extended range of wind speeds, up to 20 m/s. Furthermore, solving the complete flow field permits deeper analyses of local flow features, especially at non-nominal operating conditions, thus enabling the design of a more efficient wind turbine blade. For these purposes, a quasi-steady approach used by the k-ω SST turbulence model presents a satisfactory tool.

Nomenclature

C_l – lift coefficient, [−]
C_d – drag coefficient, [−]
C_P – power coefficient, [−]
C_T – thrust coefficient, [−]
C_m – moment coefficient, [−]
D – rotor diameter, [m]
k – turbulence kinetic energy, [m^2s^2]
M – Mach number (= v/a), [−]
P – mechanical power, [W]
R – rotor radius, [m]
Re – Reynolds number (= $\rho vc/\mu$)
T – thrust force, [W]
$u*u*$ – friction velocity, [ms^{-1}]
V_0 – wind speed, [ms^{-1}]
V_{cut} – cut-in wind speed, [ms^{-1}]
V_{out} – cut-out wind speed, [ms^{-1}]
v – velocity, [ms^{-1}]
y/R – relative longitudinal coordinate, [−]
y – nearest wall distance, [m]
y^+ – non-dimensional wall distance (= $uy/v)u*y/v$), [−]

Greek symbols

α – angle of attack, [°]
μ – dynamic viscosity, [$kgm^{-1}s^{-1}$]
θ_0 – pitch angle, [°]
ν – local kinematic viscosity, [m^2s^{-1}]
ρ – density, [kgm^{-3}]
ω – rotor rotational speed, [rpm]

References

[1] Plaza, B., *et al.*, Comparison of BEM and CFD results for MEXICO Rotor Aerodynamics, *Journal of Wind Engineering and Industrial Aerodynamics, 145* (2015), 10, pp. 115-122
[2] Shen, W. Z., *et al.*, Actuator Line/Navier-Stokes Computations for the MEXICO Rotor: Comparison with Detailed Measurements, *Wind Energy, 15* (2012), 7, pp. 811-825
[3] Kim, T., *et al.*, Improved Actuator Surface Method for Wind Turbine Application, *Renewable Energy, 76* (2015), 4, pp. 16-26
[4] Jeong, M. S., *et al.*, The Impact of Yaw Error on Aeroelastic Characteristics of a Horizontal Axis Wind Turbine Blade, *Renewable energy, 60* (2013), 12, pp. 256-268
[5] Qiu, Y. X., *et al.*, Predictions of Unsteady HAWT Aerodynamics in Yawing and Pitching Using the Free Vortex Method, *Renewable Energy, 70* (2014), 10, pp. 93-106
[6] Shen, W. Z., *et al.*, Tip Loss Corrections for Wind Turbine Computations, *Wind Energy, 8* (2005), 10-12, pp. 457-475
[7] Henriksen, L. C., *et al.*, A Simplified Dynamic Inflow Model and Its Effect on the Performance of Free Mean Wind Speed Estimation, *Wind Energy, 16* (2012), 11, pp. 1213-1224
[8] AbdelSalam, A. M., Ramalingam, V., Wake Prediction of Horizontal-Axis Wind Turbine Using Full-Rotor Modeling, *Journal of Wind Engineering and Industrial Aerodynamics, 124* (2014), 1, pp. 7-19
[9] Esfahanian, V., *et al.*, Numerical Analysis of Flow Field Around NREL Phase II Wind Turbine by a Hybrid CFD/BEM Method, *Journal of Wind Engineering and Industrial Aerodynamics, 120* (2013), 9, pp. 29-36
[10] Svorcan, J., *et al.*, Two-Dimensional Numerical Analysis of Active Flow Control by Steady Blowing Along Foil Suction Side by Different URANS Turbulence Models, *Thermal Science, 21* (2017), Suppl. 3, pp. S649-S662
[11] Bak, C., *et al.*, Description of the DTU 10 MW Reference Wind Turbine, DTU Wind Energy, Roskilde, Denmark, 2013
[12] Schepers, J. G., *et al.*, Final Report of IEA Task 29, Mexnext (Phase 1): Analysis of Mexico Wind Tunnel Measurements, ECN Wind Energy, Petten, The Netherlands, 2012
[13] Yang, X., Sotiropoulos, F., A New Class of Actuator Surface Models for Wind Turbines, *Wind Energy, 21* (2018), 5, pp. 285-302
[14] Nilsson, K., *et al.*, Validation of the Actuator Line Method Using Near Wake Measurements of the MEXICO Rotor, *Wind Energy, 18* (2015), 3, pp. 499-514
[15] Sorensen, N. N., *et al.*, Near Wake Reynolds-Averaged Navier-Stokes Predictions of the Wake Behind the MEXICO Rotor in Axial and Yawed Flow Conditions, *Wind Energy, 17* (2014), 1, pp. 75-86
[16] Zahle, F., *et al.*, Comprehensive Aerodynamic Analysis of a 10 MW Wind Turbine Rotor Using 3-D CFD, *Proceedings*, 32nd ASME Wind Energy Symposium, National Harbor, Md., USA, 2014, article number 102895
[17] Zahle, F., *et al.*, Aero-Elastic Optimization of a 10 MW Wind Turbine, *Proceedings*, 33rd Wind Energy Symposium, Kissimmee, Fla., USA, 2015, AIAA, article number 112919
[18] Marten, D., Wendler, J., *Qblade guidelines*, Ver. 0.6, Berlin, Germany, 2013

[19] Drela, M., XFOIL: An Analysis and Design System for Low Reynolds Number Air-foils, *Low Reynolds number aerodynamics Proceedings of the Conference Notre Dame*, Notre Dame, Ind., USA, 1989, Springer-Verlag Berlin, Heidelberg, pp. 1-12
[20] Fuglsang, P., *et al.*, Validation of a Wind Tunnel Testing Facility for Blade Surface Pressure Measurements, Risoe-R-981(EN), Riso National Laboratory, Roskilde, Denmark, 1998
[21] Holierhoek, J. G., Aeroelasticity of Large Wind Turbines, Ph. D. theses, Delft University of Technology, Delft, The Netherlands, 2008
[22] Wang, L., *et al.*, State of the Art in the Aeroelasticity of Wind Turbine Blades: Aeroelastic Modelling, *Renewable and Sustainable Energy Reviews, 64* (2016), 10, pp. 195-210
[23] Spalart, P., Allmaras, S., A One-Equation Turbulence Model for Aerodynamic Flows, *Proceedings*, 30th Aerospace Sciences Meeting and Exhibit, 1992, Reno, Nev, USA, AIAA, article number AIAA-92-0439
[24] Pajčin, M. P., *et al.* Numerical Analysis of a Hypersonic Turbulent and Laminar Flow Using a Commercial CFD solver, *Thermal Science, 21* (2017), Suppl. 3, pp. S795-S807
[25] *** ANSYS FLUENT Theory Guide, ANSYS, Inc., Canonsburg, Penn., USA, 2015
[26] Menter, F. R., Zonal Two Equation k-ω Turbulence Models for Aerodynamic Flows, *Proceedings*, 23rd Fluid Dynamics, Plasmadynamics, and Lasers Conference, Orlando, Fla., USA, 1993, AIAA, Article Number AIAA-93-2906
[27] Peric B., *et. al.*, Numerical Analysis of Aerodynamic Performance of Offshore wiNd Turbine, *Proceedings*, 7th International Congress of Serbian Society of Mechanics, Sremski Karlovci, Serbia, 2019
[28] Svorcan, J., *et al.*, Estimation of Wind Turbine Blade Aerodynamic Performances Computed Using Different Numerical Approaches, *Theoretical and Applied Mechanics*, *45* (2018), 1, pp. 53-65

Paper submitted: February 16, 2020
Paper revised: March 27, 2020
Paper accepted: April 1, 2020